Analytical Methods

PAPER

View Article Online
View Journal

Cite this: DOI: 10.1039/c4ay00539b

In situ characterization by Raman and X-ray fluorescence spectroscopy of post-Paleolithic blackish pictographs exposed to the open air in Los Chaparros shelter (Albalate del Arzobispo, Teruel, Spain)

Àfrica Pitarch,[ab] Juan Francisco Ruiz,[c] Silvia Fdez-Ortiz de Vallejuelo,[a] Antonio Hernanz,[d] Maite Maguregui*[e] and Juan Manuel Madariaga[a]

Received 4th March 2014
Accepted 14th June 2014

DOI: 10.1039/c4ay00539b

www.rsc.org/methods

An *in situ* study of post-Palaeolithic blackish pictographs found in an open air rock-shelter, Los Chaparros site (Albalate del Arzobispo, Teruel province, Spain), was carried out to identify the black pigments used. The composition of the pigments was analyzed by means of non-invasive instrumentation, such as a portable Raman spectrometer (RS) and a hand-held energy dispersive X-ray fluorescence (EDXRF) analyzer. In addition, some black natural deposits with a dendritic pattern, typical of manganese compounds, were also *in situ* analysed with the aforementioned techniques to explore the possibility that post-Paleolithic people used minerals from the surroundings of the Los Chaparros rock-shelter to elaborate the paintings. The results obtained by the EDXRF analyses of black pigments showed differences in composition between a black Levantine deer, in which manganese was present as the main element, and a deep red Schematic pictograph that included manganese as the secondary element. The results of Principal Component Analysis (PCA) of collected EDXRF spectra showed similarities in the elemental composition between the manganese dendrite formations present in the rock-shelter and the black deer. In order to confirm this, the *in situ* analytical campaign was completed with some analysis in the laboratory by using micro-RS (μ-RS) and X-ray diffraction (XRD) on mineral samples having black crystallisations. Two specimens were taken, one from the black dendrite present in the same rock-shelter and the other from the Los Mases de Crivillén mining area (which is near to Los Chaparros). These analyses revealed that the characteristic bands of Mn–O and Mn–OH bending and stretching vibrations obtained *in situ* on the black pictograph were the same as those observed in the Raman spectra of the dendrite mineralization of Los Chaparros obtained in the laboratory by μ-RS.

Introduction

Rock art pictographs of the Los Chaparros site (Albalate del Arzobispo, Teruel province, Spain) were discovered in 1985.[1] It was one of the rock art sites included in the UNESCO World Heritage List in 1998, under the generic denomination of Rock Art of the Mediterranean Basin of the Iberian Peninsula. The rock art imagery was painted in a calcareous rock-shelter where remarkable examples of Levantine and Schematic styles of the Iberian Peninsula have been preserved. Until now, 115 pictographs have been described but the shelter is under revision and it is expected to identify new ones. The largest part of the paintings was made in reddish shades, ranging from deep red to light red. However, one black Levantine figure and a very dark red of Schematic style attracted our attention because they cannot be clearly related to the rest of the pictographs of this site.

Black pigments found in rock art all around the world are usually organic carbon bearing pigments (such as charcoal, soot

[a]*Department of Analytical Chemistry, Faculty of Science and Technology, University of the Basque Country UPV/EHU, P.O. Box 644, 48080 Bilbao, Spain*

[b]*GRAPAC-UAB ("Grup de Recerca Aplicada al Patrimoni Cultural"), Research Group Attached to the Department of Animal Biology, Plan Biology and Ecology, Faculty of Biosciences, Autonomous University of Barcelona (UAB), 08193 Bellaterra, Barcelona, Spain*

[c]*Departamento de Historia, Área de Prehistoria, Facultad de Ciencias de la Educación y Humanidades, University of Castilla-La Mancha (UCLM), Avda. de los Alfares 42, 16002 Cuenca, Spain*

[d]*Dpto. de Ciencias y Técnicas Fisicoquímicas, Facultad de Ciencias, Universidad Nacional de Educación a Distancia (UNED), Paseo Senda del Rey 9, 28041 Madrid, Spain*

[e]*Department of Analytical Chemistry, Faculty of Pharmacy, University of the Basque Country UPV/EHU, P.O. Box 450, 01080 Vitoria-Gasteiz, Spain. E-mail: maite.maguregui@ehu.es; Tel: +34 94 501 30 58*

and bone black) and manganese oxyhydroxides or iron oxyhydroxides.[2–4] Manganese oxides present several mineralogical forms on the earth's surface (mineralogists have identified more than 30 $Mn_xO_y(OH)_z$) that can be distinguished according to their chemical composition, oxidation degree-Mn^{2+}, Mn^{3+}, Mn^{4+} or mixed- and crystalline structure – in tunnels of various sizes, the bigger ones containing cations or water molecules, in layers or in spinel;[5,6] some of them are of black shade. Magnetite (Fe_3O_4) is the most representative black compound among the different iron oxyhydroxides.

Inside the rock-shelter of Los Chaparros, there are black natural deposits with a dendritic pattern, typical of manganese compounds. The dendrite formation process is quite simple involving the mobilization of manganese by means of water surface. This mobilization affects other metals, leading to the precipitation of complex mixtures of oxides and, thus, originating in a manganese dendrite specimen with a high degree of chemical heterogeneity. These kinds of mineralization may be on the rock surface, along fracture surfaces of the rock or within the rock matrix. Although these mineralizations have long been considered to be of pyrolusite, no example of this mineral has yet been identified. According to the literature,[7] the manganese minerals present in the dendrites are usually romanechite $(Ba,H_2O)_2Mn_5O_{10}$ or one of the following hollandite-group minerals: hollandite ($BaMn_8O_{16}$), cryptomelane (KMn_8O_{16}) or coronadite ($PbMn_8O_{16}$).

Moreover, Los Chaparros shelter is located in the region of Las Cuencas Mineras ("Mining district") of Teruel province (Fig. 1) which has a well documented mining history, exploiting and producing lignite, iron, lead and salt, among other minerals. Research in the mining archives[8,9] has documented a possible source area of the black powder (pigment) in a manganese exploitation, located in Los Mases de Crivillén area, 40.5 km south of the site of Los Chaparros. The ore is associated with karstic cavities developed on stratiform carbonate materials of Aptian age. Mineralization consists of filling cavities materials, composed of pyrolusite (MnO_2), birnessite [$(Na,Ca,K)_x(Mn^{4+},Mn^{3+})_2O_4\cdot 1.5(H_2O)$], manganite [MnO(OH)], romanechite [$(Ba,H_2O)_2Mn_5O_{10}$] and todorokite [$(Na,Ca,K)_2(Mn^{4+},Mn^{3+})_6O_{12}\cdot 3–4.5(H_2O)$] with associated goethite [FeO(OH)], hematite [Fe_2O_3] and calcite [$CaCO_3$] minerals.[10,11]

The aim of the research on these black and deep red pigments was twofold: firstly to characterize the nature of the black pigments used in the two aforementioned prehistoric depictions, and secondly to explore the possibility that post-Palaeolithic people used minerals from the surroundings of Los Chaparros rock-shelter to elaborate the paintings. Our investigation in Los Chaparros was included in the Mic-Raman Prehistoria multidisciplinary research project (id. CTQ2009-12489), carried out from 2010 to 2012. This project used *in situ* spectroscopic techniques in order to identify the physical chemical composition of paint recipes, bedrocks and accretionary coatings associated with rock art pictographs. A group of ten sites distributed over four Autonomous Communities of Spain were selected for this purpose. Red, white and black pictographs of Levantine and Schematic styles were preserved in this group of

Fig. 1 Geographical location of the Los Chaparros site (Albalate del Arzobispo, Teruel province, Spain).

rock art sites. Many of them were good examples of these prehistoric arts and were selected as a significant sample of the typical problems posed by stylistic variability in this group of open-air rock art shelters. In this regard, the use of non-invasive portable instrumentation was the unique option to get a relevant amount of information about the nature and the structure of materials avoiding collection of samples and any contact with the painting surface.[12] Our aim was also to redefine relationships between pictorial stages based on the physico-chemical identity of pictographs instead of using style as a self-explanatory concept based on preconceived ideas about prehistoric art chronological frameworks.

To continue with the previous studies, we adopted a multi-spectroscopic approach in Los Chaparros by using two non-invasive techniques. The first analytical step was the *in situ* examination of the rock paintings without taking any sample by means of a hand-held energy dispersive X-ray fluorescence (EDXRF) analyzer, to identify the pigments through the detection of their chemical elements. After this screening phase, to complete the fieldwork a portable instrument based on Raman spectroscopy (RS) was used to obtain the necessary molecular information to properly characterise the studied rock art.

In analytical chemistry, archaeometry and conservation, the use of chemometric methods, such as principal component

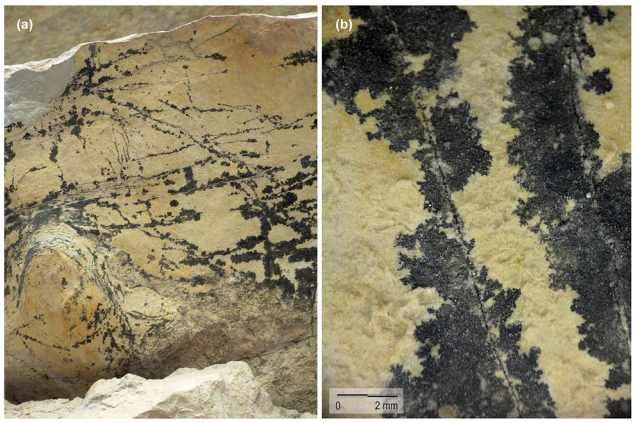

Fig. 2 Dendrite formations in the ceiling of the shelter near to the point where the deer is preserved. (a) General view; (b) micropicture 10× of this dendrite formation.

analysis (PCA) and hierarchical clustering (HC), are usually with values of concentrations present in the samples.[13–15] In this study, EDXRF spectral data obtained *in situ* combined with multivariate data analysis were applied to the study of the samples since these kinds of studies allow the extraction and visualization of a much larger amount of information.[16,17] Furthermore, the *in situ* analytical campaign was completed with some analysis in the laboratory on mineral samples having black crystallisations. Two specimens were taken, one from the black dendrite formation present in the same rock-shelter (Fig. 2) and the other from Los Mases de Crivillén mining area, in order to know if those natural deposits from the surrounding of Los Chaparros rock-shelter could have been used as raw materials to elaborate the black pigment. These samples were analyzed using micro-RS (μ-RS) laboratory instruments in order to obtain the maximum spectral information at the micrometric level. In addition, X-ray diffraction (XRD) was also employed to obtain information about the existing crystalline phases.

Materials and methods

Los Chaparros rock art site

The rock art site of Los Chaparros is located in the northwestern part of Sierra de Arcos range. This broad rock-shelter is placed in the base of a huge cliff, in the upper part of a deep canyon of stepped sides. The Martín River, which runs through this gorge, has shaped the lower Jurassic limestones known as Formación Cuevas Labradas for millennia.[18,19] This rock-shelter is characterized by several cavities/entrances subjected to direct solar radiation, thermal changes and rain. In this context several pictographs related to Schematic and Levantine art and depicting human shapes and zoomorphic figures are arranged.[20] Levantine figures of this shelter include animals like deer, horses, wild boars and wild goats; human figures are mainly archers but there is a depiction of a pregnant female as well. Several hunting and fighting scenes can be appreciated. Among the Schematic arts of this site there are several tree-like forms, zigzags, spirals, deer, and horses. In some cases it is very hard to decide if some of these animals are of Levantine or Schematic styles.

Amongst its 115 parietal motifs, the painting ensemble contains at least one black figure and a very deep red one that are specifically studied in this paper. The black figure is the depiction of a stag of Levantine style (see Fig. 114)[1] that is located in the left hand area of the shelter. Only the forepart of the animal is preserved, including the two front legs, long neck, chest, head and antlers. It was executed with a broad contour line and filled with a striated pattern. All the brushstrokes of this figure are of a regular width and were made with a black paint (Fig. 3).

The deep red is a tree-like Schematic figure that was not recorded by the first researchers of Los Chaparros. However, it is clearly visible. It is composed of three vertical parallel lines and at least six short upward lateral branches on the left and three on the right. This figure resembles other tree-like forms of this shelter; Fig. 14, 15, 17 and 25 in ref. 1 show a similar structure of vertical lines with short lateral branches, and could be among the older pictographs of this site (see Fig. 15).[1] The deep red one is clearly darker than the other tree-like forms and it was made with broad brushstrokes, typical of Iberian Schematic art (Fig. 4).

Methods

***In situ* analyses.** The screening elemental analyses were performed by using a hand-held X-MET5100 EDXRF spectrometer (Oxford Instruments, UK) equipped with a rhodium anode

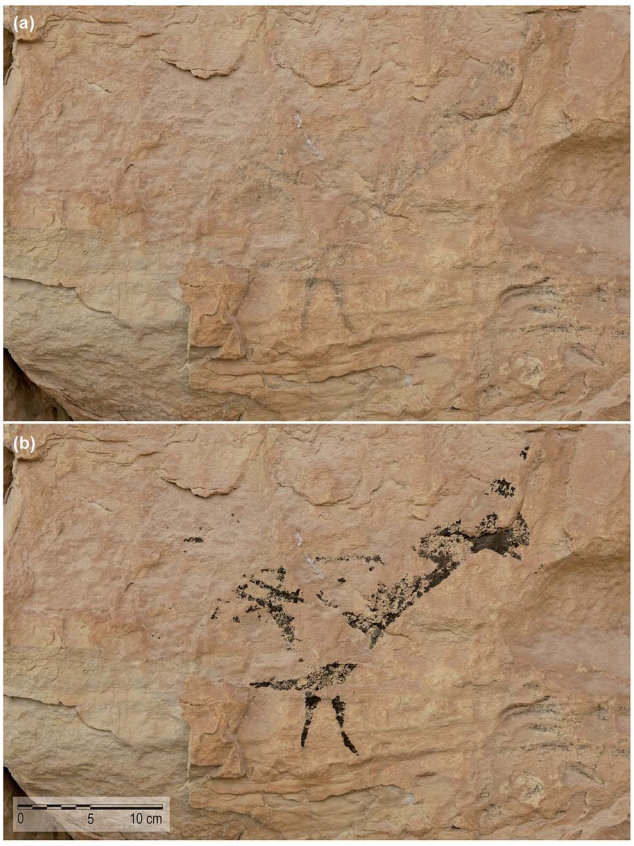

Fig. 3 Black Levantine deer. (a) Current conservation state of the pictograph and (b) digital tracing superimposed over the picture.

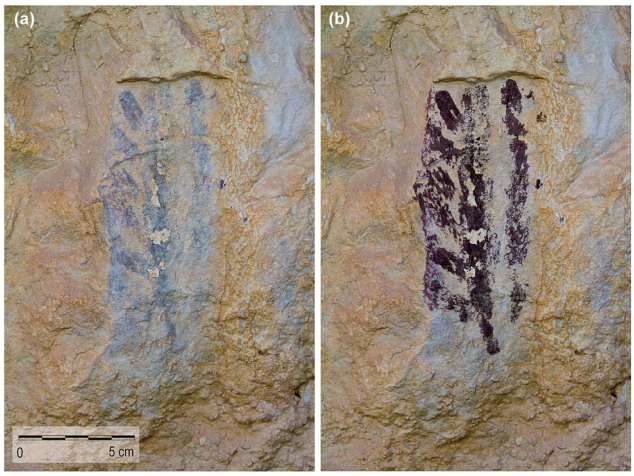

Fig. 4 Red deep Schematic tree-like motif. (a) Current conservation state of the pictograph and (b) digital tracing superimposed over the picture.

X-ray tube (operating at 45 kV). The size of the X-ray beam in the used instrument is 9 mm. The analyser has a high resolution silicon drift detector (SDD), with the spectral resolution being 20 eV and the energy resolution around 150 eV (calculated at the K-alpha line of Mn at −20 °C). The instrument is also equipped with a Personal Digital Assistant (PDA) that allows an easier management of the instrument. The measurements were taken in 50 seconds counting time. The *in situ* Raman analyses were carried out with a portable InnoRam spectrometer (B&WTEK-INC., Newark, USA) equipped with a 785 nm diode laser. The spectrometer worked in a spectral range from 65 to 2500 cm^{-1}. The maximum laser power of the system is 300 mW at excitation port. The laser power was adjusted *via* neutral density filters from 100% to 1% of the total power. In order that the crystalline structure of the compounds present in the dendrite mineralization and in the black painting of the panel is not modified, the laser output power used to analyze these areas never exceeded 9.5 mW measured at the focus position of the probe head (10×). Spectra acquisition was done with the software BWSpec™ 3.26 (Newark, USA). The spectra were recorded with an integration time varying from 0.5 to 10 seconds, in a spectral range from 100 to 2200 cm^{-1} and with a number of accumulations varying between 20 and 200 (depending on the case of analysis, the presence of fluorescence radiation and the signal-to-noise ratio). The obtained Raman spectra were processed by the Nicolet Omnic 7.2 software (Madison, Wis., USA) and the identification was based on a comparison of the recorded spectra with those of several spectra databases.[21,22]

Chemometric data treatment. In the dataset of the EDXRF spectra, the first step consisted in choosing the most appropriate spectral region. In our case no significant differences were found in selecting different regions, thus the whole region from 0 to 40 keV was considered. Also spectral treatments were used such as spectral normalization, mean and center. The final dataset included 21 samples or number of acquired spectra (7 on black Levantine Fig. 4 on deep red of schematic style, 6 on dendrite mineralization and 4 on rock-substrate) and 2048 variables (keV).

Principal Component Analysis (PCA) was applied to the EDXRF spectra using the software Matlab 2010 with PLS Toolbox, version 7.0.2 from Eigenvector Technologies (Massachusetts, USA).

Laboratory instrumental setup. The Raman study carried out at the laboratory was done with two equipment. The first one is a Renishaw RA100 Raman microprobe spectrometer (Renishaw, Gloucestershire, UK) equipped with 20× and 50× long-range objective lenses mounted in the head of the Raman microprobe with a micro-video camera, a 785 nm wavelength diode laser excitation source (nominal laser power 300 mW) and a Peltier cooled CCD detector. The instrument was calibrated using the 520 cm^{-1} Raman band of a crystalline silicon chip. Spectra were recorded from 100 to 2200 cm^{-1} with an integration time ranging from 5 to 20 s for each spectrum, and with a number of accumulations varying between 10 and 30 times in order to improve the signal-to-noise ratio. Laser power on the sample surface was also controlled using neutral density filters and it never exceeds 3 mW when dendrite mineralizations were analyzed. Spectral acquisition was performed using the Wire 3.2 software.

The second Raman equipment was a Horiba Jobin Yvon LabRam-IR HR-800 spectrograph coupled to an Olympus BX41 microscope. In this last case, the measurements were carried out following procedures described elsewhere.[23] The interpretation of the laboratory Raman results was again performed by comparing the acquired spectra with the spectra of pure standard compounds collected in diverse databases.[21,22]

It is necessary to remark that the lateral spatial resolution (XY) of the two laboratory Raman instruments and the portable Raman spectrometer used during the field work ranges between 430 and 1900 nm and the axial resolution of the three instruments ranges between 0.6 and 2 μm. Both values depend on the laser wavelength and the objective used for each measurement.

Structural analyses were carried out by X-ray diffraction, using a Philips Xpert PRO diffractometer (PANalytical) with a Cu Kα target tube X-ray source ($\lambda Cu_{K\alpha average}$ = 15 418 Å, $\lambda Cu_{K\alpha 1}$ = 154 060 Å and $\lambda Cu_{K\alpha 2}$ = 1 544 398 Å, operating at 40 kV and 40 mA) and a PixCel detector. The angular range (2θ) was explored using a vertical goniometer (Bragg–Bretano geometry) scanning from 5° to 69°, at a step size of 0.02°. Evaluation of X-ray diffractograms was performed by using the routines of the X'pert HighScore software package (PANalytical) combined with the specific powder diffraction file (PDF2) database (International Centre for Diffraction Data – ICDD, Pennsylvania, USA). The crystalline phase analyses were carried out in two ways: (1) mounting the entire fragment on a mobile plate stage to adequately align the system, without previously preparing the sample; and (2) mounting few micrograms of the powdered sample (grinded in an agate mortar) on a silicon sample holder.

Results and discussion

As revealed by the spectral data obtained by *in situ* EDXRF analyses, the presence of calcium, iron, manganese and

strontium is really important among the different elements. Ca is extensively distributed all over the rock surface, coming from the bedrock underneath, as it will be described below. The presence of Sr in the spectra is linked with Ca, since it is usually present in the calcite/dolomite crystalline lattice. Ca presence in the EDXRF spectra can also be related to calcium oxalate compounds, as it will be described later. In previous studies related to the characterization of the micro-stratigraphy of the Los Chaparros rock-substrate,[24] it was observed that the maximum thickness of the oxalate patina in the analyzed polished thin sections was set around 200 μm. It is well-known that the oxalate patina on rock-shelters could be very heterogeneous, thus the thickness can vary on each measurement. In the literature, the maximum thickness of oxalate patina found on rock-shelters is set more or less as 500 μm. Moreover, previous microscopic observations of the pigment remains present on the Los Chaparros panel indicate that the pigment layer thickness ranges between 5 and 50 μm. The X-ray beam penetrates some millimetres, but the EDXRF analysis offers information of the elemental composition of superficial layer with thicknesses lower than 1 mm, since the fluorescence radiation from the elements of the sample have lower energy than the incident beam. Considering that the thickness of the oxalate patina and pigment remains is around 250 μm, it is supposed that the EDXRF analysis offered us information about the oxalate patina, pigment remains and the substrate at the same time. Therefore, the EDXRF analysis on pictograph can give simultaneous information of the oxalate patina, pigment layer and rock substrate.

In the EDXRF analysis of the deep red motif showed higher presence of iron than the first pictograph and the rock substrate (Fig. 5). The presence of some elements is higher in the blackish pictographs and the dendrite mineralization than its amount in the rock substrate; this is the case of Pb, Zn and Ba (see Fig. 5). The presence of Ba has been confirmed in the EDXRF spectra through the detection of their K-alpha line at 32.19 keV fluorescence line.

The highest contents of manganese are restricted to dendrite formation, although the black and the deep red figures also present a relevant amount of manganese (Fig. 5 and 6). The EDXRF analysis of the deep red motif showed higher presence of iron than the black pictograph and the rock substrate (Fig. 6). In the Raman analyses performed on the deep red pigment, the high amount of fluorescence obscured the Raman signals, the extraction of Raman bands related with the deep red pictorial recipe being impossible. Additional Raman measurements were performed in the vicinity of the deep red pictograph (see Fig. 7) obtaining Raman bands at 226, 294, 411, 499, 616 and 1294 cm^{-1}, which can be assigned to hematite. Moreover, hematite was also clearly identified by *in situ* Raman analyses in a group of red Schematic finger stencils present in other areas of the same shelter (see Fig. 1c in ref. 24). The high contribution of iron in the deep red paint and the presence of hematite close to this pictograph may suggest that hematite could be included in the deep red pigment. In the same Raman spectrum acquired in the vicinity of the deep red pictograph, additional bands at 570 and 669 cm^{-1} that could be assigned to manganese oxide were also detected (see Fig. 7). In this particular case, these two Raman bands can be the two most important features of chalcophanite ($ZnMn_3O_7 \cdot 3H_2O$), a black compound found in the dendrite of the shelter, as it will be shown later. Moreover, the

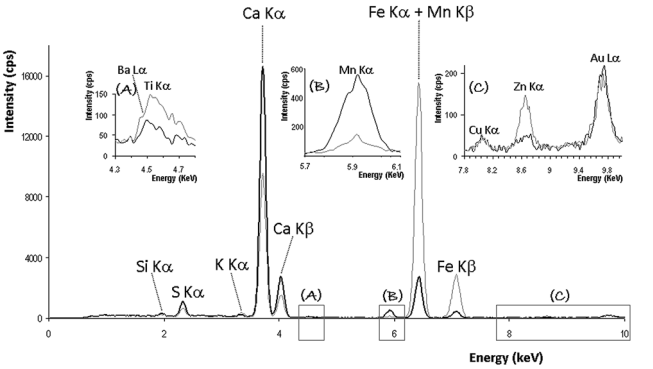

Fig. 6 *In situ* EDXRF spectra of black Levantine figure (solid black line) and deep red of Schematic style (solid grey line).

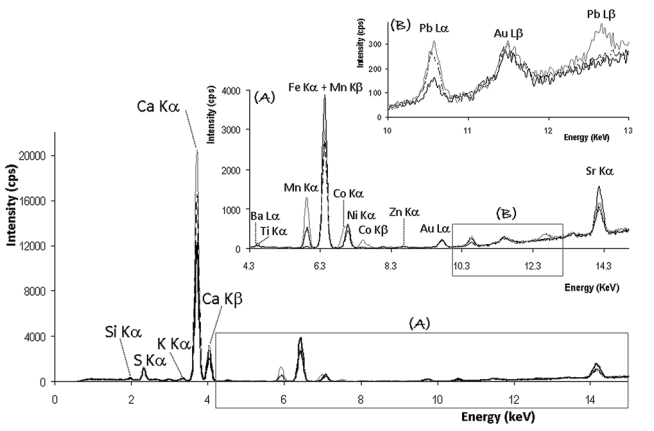

Fig. 5 *In situ* EDXRF spectra of rock substrate (solid black line), dendrite mineralization (solid grey line) and black painting (dotted line).

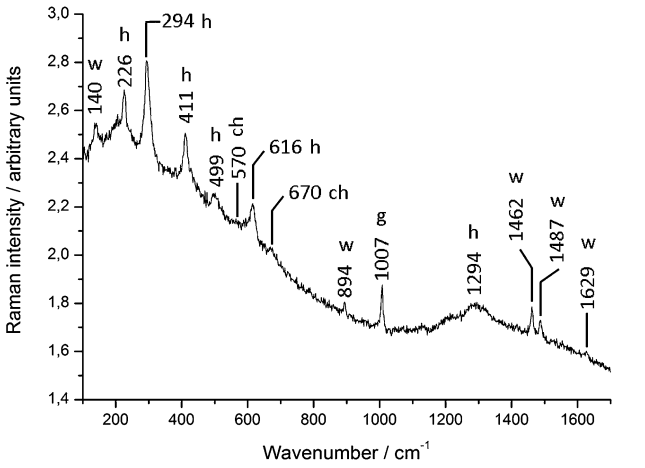

Fig. 7 *In situ* Raman spectrum of a red painting from Los Chaparros. Labels: h, hematite; w, whewellite; g, gypsum; and ch, chalcophanite.

element Zn has been detected in the EDXRF analysis of both, the deep red pictograph and the dendrite mineralization (see Fig. 6).

In order to undertake a preliminary investigation of the source of the manganese in the two figures, EDXRF spectra of the rock substrate, of the dendrite mineralization and of both pictographs were subjected to chemometric treatment *via* PCA.

All the spectral data (21 analysis × 2048 variables) were finally mean and centered. Fig. 8a and b show PC1 × PC2 × PC3 scores and loading plots, where the 3 first PCs account for 97.97% of the total variance (PC1: 51.27%, PC2: 37.57% and PC3: 9.90%). In the scores plot, in general, a separation into three groups is observed corresponding to the rock substrate (PC1 > 0), the deep red motif (PC1 < 0) and the dendrite mineralization plus the black Levantine deer (PC1 < 0). This separation is mainly due to 3.7 keV (K-alpha characteristic line for Ca) with positive PC1 and PC2, 5.9 keV (K-alpha characteristic line for Mn) with negative PC1 and negative PC2, and 6.4 keV (K-alpha characteristic line for Fe) with negative PC1 and positive PC2. In summary, Fe, Ca and Mn have a significant influence for PC1 and PC2 loading, as shown in Fig. 8b. The measurements done in the figures are distributed in different groups in scores plot of PC1/PC2. This can be ascribed to the different chemical composition of the paint of the second figure, where the manganese concentration was present in lower levels in comparison to the iron red pigment. Although it is clear that the first black figure and the dendrite mineralization showed similar characteristics of the measured elements, the chemometric results suggest but are not conclusive enough to assure that the raw materials used for the elaboration of the black pigment are related to the local dendrite mineralization.

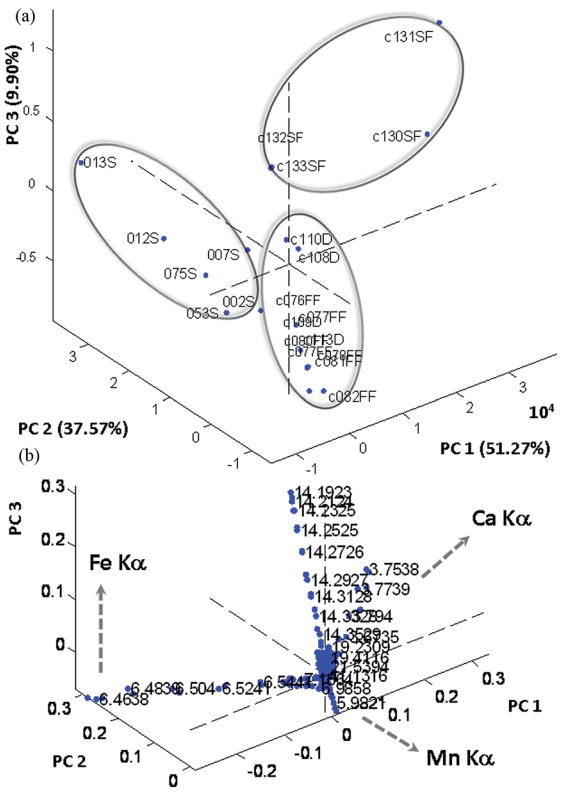

Fig. 8 (a) Scores plot of PC1/PC2/PC3 and (b) Loadings plot of PC1/PC2/PC3 of the 21 EDXRF spectra recorded in Los Chaparros panel (S: rock substrate, FF: first figure, black deer, SF: second figure, dark red motif and D: dendrite mineralization).

According to the Raman analyses of the rock substrate (not shown), the presence of dolomite ($CaMg(CO_3)_2$, Raman bands at 301, 1096 cm^{-1}) and calcite ($CaCO_3$, Raman bands at 281, 712 and 1085 cm^{-1}) was corroborated. Furthermore, on the rock surface the presence of gypsum ($CaSO_4 \cdot 2H_2O$, Raman bands at 414, 493, 669, 1007 and 1027 cm^{-1}) was identified and, in some cases, also showed the presence of anhydrite ($CaSO_4$) due to its characteristic band at 1015 cm^{-1}, probably due to the gypsum dehydration process. In addition, the presence of whewellite ($CaC_2O_4 \cdot H_2O$, main Raman bands at 1462 and 1488 cm^{-1}) together with weddellite ($CaC_2O_4 \cdot 2H_2O$, main Raman band at 1475 cm^{-1}), both of them being hydrated forms of calcium oxalate, was also detected along the analyzed surface of the rock-shelter.

Calcium oxalate coatings are frequently found on this kind of environments and there are several hypotheses on their origin/presence, ranging from results of human activity (e.*g.* whewellite could be added when plant sap was used as binder, extender of whitener[25,26]) to metabolic action of lichens, bacteria, fungi, algae and microbes inhabiting the outer layers of rock faces.[27–33] According to the literature, these microorganisms could excrete the oxalic acid, which reacts with the calcium compounds of the surroundings such as calcite/dolomite of the rock substrate or the gypsum of the surface, leading to the formation of calcium oxalate.[34] Another hypothesis states that the oxalic acid could be related to the chemical decomposition of the binding media employed for the elaboration of the pictographs due to the feeding action of microorganisms,[35,36] hypothesis that was discarded for this rock-shelter since these compounds are widely distributed all over the rock surface. In reference to the characterization of the dendrite formation, *in situ* Raman analysis (Fig. 8a) revealed the presence of dolomite (main Raman band at 1096 cm^{-1}), gypsum (Raman bands at 669, 1007 and 1027 cm^{-1}) from the rock substrate and whewellite from the rock surface (Raman bands at 895, 1462 and 1488 cm^{-1}). Furthermore, a few weak bands appeared in the spectral range of 500–700 cm^{-1}, characteristic of Mn–O and Mn–OH bending and stretching vibrations. Regarding the black painting (Fig. 9b), once again *in situ* Raman analyses gave highly resolved spectra showing the presence of dolomite, gypsum (Raman bands at 414, 493, 669, 1007 and 1027 cm^{-1}) and whewellite (Raman bands at 140, 195, 206, 220, 248, 500, 519, 895, 1462, 1488 and 1627 cm^{-1}). No bands in the range between 1300 and 1600 cm^{-1} were identified, so that the presence of carbon bearing pigments can be excluded.

A detailed view of a representative spectrum, in the region of 500–700 cm^{-1}, for the case of the dendrite mineralization is shown in Fig. 10a(i), where several Raman bands are revealed at about 544, 566, 588, 591, 614, 620 and 644 cm^{-1}. Another representative Raman spectrum of the black pictograph shown in Fig. 3 also exhibits the weak and broad bands observed in the former spectra (see Fig. 10a(ii)). The closeness of both spectra,

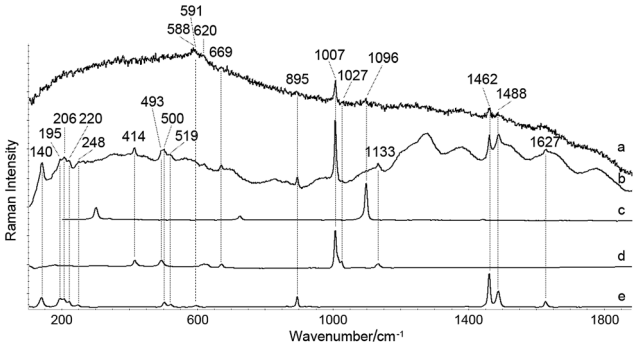

Fig. 9 *In situ* Raman spectra of (a) manganese dendrite mineralization and (b) black painting (obtained by using the portable Raman spectrometer with the laser line at 785 nm). The reference spectra of dolomite (c), gypsum (d) and whewellite (e) spectra are displayed for comparison in the inset.

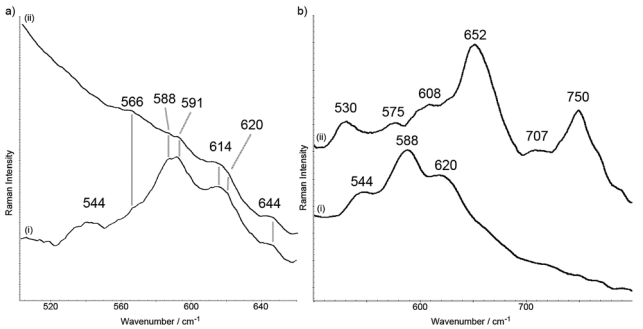

Fig. 10 (a) *In situ* Raman spectra of (i) manganese dendrite mineralization and (ii) black painting (obtained by using the portable Raman spectrometer with the laser of 785 nm); (b) *ex situ* μ-RS spectra of (i) sample of manganese dendrite mineralization and (ii) specimen taken from Los Mases de Crivillén manganese mining area (obtained by using the laboratory Raman spectrometer with the 785 nm laser line).

taken *in situ* with a spot size of nearly 100 μm, suggests the use of a pigment with a chemical composition similar to the black material found in the dendrite formations of the shelter to execute the deer motive. Several compounds are simultaneously present in the two spectra shown in Fig. 10a:

• Manganese(II) oxide (MnO) only in the dendrite spectrum, the less oxidised form of manganese, with its characteristic Raman bands at 544 and 644 cm^{-1},[22]

• Cryptomelane ($K_2Mn_8O_{16}$), a compound consistent with the identification of potassium in the XRF analysis of both the dendrite and the black pigment (see Fig. 5 and 6), showing its main Raman band at 644 cm^{-1},[37]

• Coronadite ($PbMn_8O_{16}$), another compound consistent with the positive XRF identification of lead in both black mineralisations (see Fig. 5), with its main Raman bands at 566 cm^{-1},[22]

• Hollandite ($BaMn_8O_{16}$) could possibly be identified thanks to its main Raman band[22] at 588 cm^{-1} and to the presence of Ba in the XRF spectra of both samples (see Fig. 6),

• Marokite ($CaMn_2O_4$) could be assigned thanks to the 620 cm^{-1} band, the only one close to the expected 623 cm^{-1} one for the Mn(III) compound.[22] The other two bands at 591 and 614 cm^{-1} do not belong to manganese oxides but to whewellite (591 cm^{-1} after[30]).

The analyses at the laboratory by μ-RS allowed us to better define these Raman bands of the dendrite formation (Fig. 10b(i)) and to discard the specimen taken from Los Mases de Crivillén manganese mining area as a pigment used in the studied pictographs since its main Raman bands at about 530, 652 and 750 cm^{-1} did not correspond neither with those described *in situ* in the dendrite formation nor in the black painting (Fig. 10b(ii)); these three bands from the Los Mases de Crivillén specimen may be adscribed to ramsdellite (MnO_2, Raman bands at 526, 654 and 750 cm^{-1}) although that at 654 should be less intense (see Fig. 1B[38]), indicating probably the presence of Mn_3O_4 (hausmannite) as the band at 650 cm^{-1} is described like its most intense one.[39] Thus, the specimen taken from Los Mases de Crivillén can be a mixture of ramsdellite and hausmannite, two mineral phases of manganese oxides not detected in the *in situ* Raman spectra collected on the black pigment under study in this work.

The scientific investigation on the use of manganese compounds in rock art has been faced by means of different approaches.[2–5,40–45] In the last few years, it has been carried out with RS,[37,46–50] however determination of these compounds by means of *in situ* RS can pose quite a challenge since, as shown above, no clear Raman signature is obtained probably because of the low Raman activity of the manganese-based pigments.[39] In addition, as the laser beam spot used *in situ* was pretty large, what we often obtained was the information about the main compounds of the substrate rather than the information about the pigment and dendrites.

In order to better characterize the possible manganese oxyhydroxides present in Los Chaparros bedrock, μ-RS laboratory equipment was used. The μ-RS analysis of the specimen taken from different spots of the manganese dendrite formation (Fig. 11) allowed us to obtain several spectra with different Raman bands, what suggests its high degree of chemical heterogeneity at the micrometric level. The bands at 544 and 644 cm^{-1} (also seen in the *in situ* analysis shown in Fig. 10a) could be assigned to MnO while that at 550 cm^{-1} could be the most intense band of groutite [MnO(OH)].[22] Other compounds clearly seen are marokite (main Raman band at 620 cm^{-1}) and hollandite (main signal at 588 cm^{-1}) also observed in the *in situ* analyses.

The assignment of the other bands is rather difficult because probably several compounds are present in the same spectrum and there is not a clear consensus on the characteristic features of the different single and mixed oxidation states of manganese oxides. However, it seems that α-MnO_2 and β-MnO_2 are not present due to the absence of its most important Raman bands[38] while romanechite [$(Ba, H_2O)_2Mn_5O_{10}$] seems to be clear in Fig. 11b (ref. 47) due to its two important Raman bands at 585 and 627 cm^{-1}, as well as chalcophanite due to the 566 and 664 cm^{-1} bands (see Fig. 11c).

The spectrum shown in Fig. 11b has an important contribution of gypsum and anhydrite due to the mixed broad band at 1018 with a shoulder at 1008 cm^{-1} (wavenumbers not shown in

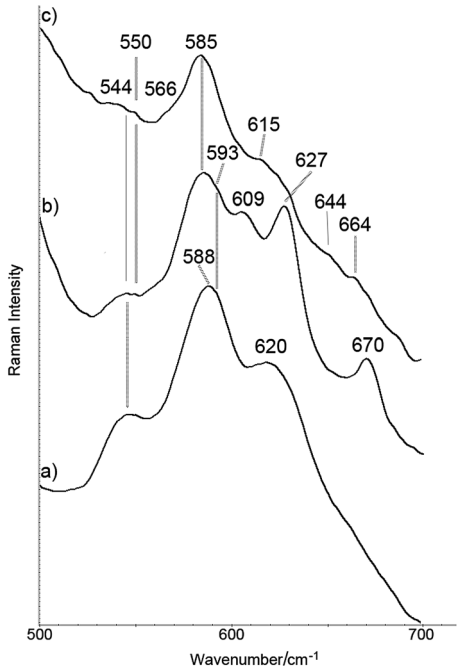

Fig. 11 μ-Raman spectra of different areas of the manganese dendrite mineralization specimen (obtained by using the laboratory Raman spectrometer with the 785 nm laser line).

Fig. 11). Thus, the bands at 609, 620 (included in the broad band at 627) and 670 cm^{-1} do not correspond to any manganese compound but to the mixed calcium sulphates.

Finally, the spectrum shown as Fig. 11c can be considered a mixture of both (a) and (b) (this spectrum without the contribution of the mixed calcium sulphates), indicating how the different manganese compounds can be present simultaneously even at the microscopic level.

The XRD analyses of the whole dendrite fragment (Fig. 12a) confirmed the presence of dolomite together with gypsum and whewellite identified by RS and the presence of quartz (SiO_2) was also revealed. In this case, it was not possible to identify the mineral phases composing the manganese mineralization. It is true that the peak at about $2\theta = 21.3°$ could suggest the presence of groutite [MnO(OH)], but a single peak is not enough to identify a mineral phase with certainty. Dealing with the XRD analysis of the fine powdered dendrite (Fig. 12b), apart from the already mentioned mineral compounds, the diffractogram revealed the presence of clay minerals (mica group and kaolinite-serpentine group). In this diffractogram, the peaks at $2\theta = 9.1°$ and $2\theta = 18.4°$ may suggest the presence of todorokite [$(Na,Ca,K)_2(Mn^{4+},Mn^{3+})_6O_{12}\cdot 3–4.5(H_2O)$], however we are not able to do a clear attribution since the rest of its reflections could be overlapped or hidden by the reflections of the main mineral phases. According to the literature, identifying the particular mineral(s) in a manganese oxide specimen by X-ray diffraction may be extremely difficult.[6,7] In this case, both the finely particulate and low crystallinity of manganese minerals comprising the dendrite specimen, as well as the presence of other mineral phases as major components of the deposits, did not allow us to identify the manganese mineral phases.

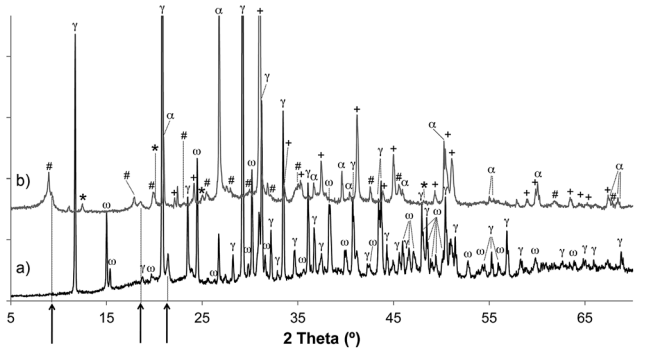

Fig. 12 Diffractograms of the manganese dendrite mineralization: (a) XRD spectra of the entire specimen (in black) and (b) XRD spectra of the powdered specimen (in grey). Key: #: muscovite (mica group); *: kaolinite (serpentine group); +: dolomite; α: quartz; γ: gypsum and ω: whewellite. The main peaks of groutite and todorokite are highlighted with arrows.

Conclusions

The combined use of hand-held/portable spectroscopic techniques such as EDXRF and RS used for *in situ* analysis of the rock substrate and paintings from Los Chaparros proved to be extremely useful for this purpose.

Thanks to the use of RS it was possible to affirm that the rock substrate is composed mainly of dolomite and calcite. Moreover, gypsum and anhydrite crystallisations were also identified, suggesting the dehydration process of the newly formed gypsum into anhydrite. Coatings of oxalates, probably originated due to the metabolic activity of microorganisms, including whewellite and weddellite crystals were also detected using this technique.[23]

Regarding the pigment of the two figures analysed in Los Chaparros rock-shelter, carbon was not detected during the *in situ* screening with the portable RS. Nevertheless, Raman bands related to Mn–O and Mn–OH bending and stretching vibrations were detected. In the same rock-shelter, manganese dendrite formations are present. Raman spectra obtained *in situ* from those manganese dendrite mineralizations also exhibit Raman bands related to Mn–O and Mn–OH bonds and fit quite well with the Raman feature of the Mn–O and Mn–OH region obtained *in situ* on these two figures. Moreover, most of the manganese mineral phases that are related to dendrite formations in the literature, have been found in this work, like hollandite ($BaMn_8O_{16}$), romanechite (Ba, $H_2O)_2Mn_5O_{10}$, coronadite ($PbMn_8O_{16}$), cryptomelane (KMn_8O_{16}), chalcophanite ($ZnMn_3O_7\cdot 3H_2O$) and groutite [MnO(OH)].

Additionally, Raman measurements were also performed on Mn-bearing minerals from Los Mases de Crivillén, relatively close to Los Chaparros shelter. The Raman measurements performed on this mineral showed some bands in the Mn–O and Mn–OH region, belonging to ramsdellite and hausmannite, which are not present in the measurements performed on the paintings from Los Chaparros rock-shelter. These results suggest that the painters could use a manganese black of a more local origin, like that identified in the dendrite mineralizations of Los Chaparros.

It is necessary to remark that the laboratory μ-Raman analyses revealed that the dendrite formation from the Los Chaparros studied *in situ* shows a high degree of chemical heterogeneity, since different Raman bands related to Mn-bearing oxides and/or oxyhydroxides were identified. XRD analyses performed on the dendrite sample (fragment and fine powdered) suggest a possible presence of oxides and oxyhydroxides such as groutite and todorokite, but its real presence cannot be confirmed due to the presence of other mineral phases as major components and the low crystallinity of Mn-bearing minerals. These results demonstrate that it is very hard to determine the specific nature of the oxides/oxyhydroxides present in both the black pigment remains and dendrites using not only RS but also XRD.

EDXRF results showed that the highest manganese content is located in the dendrite formation, although both figures also present relevant concentrations of manganese. Chemometric treatments of the EDXRF spectra (rock substrate, two pictographs and dendrite mineralization) based on principal component analysis showed that three differentiate groups (rock substrate, deep red pictograph, and dendrite mineralization + black Levantine motif) are present due to differences in the Kα lines of Ca, Fe and Mn. The deep red pictograph was made with a different paint that included iron oxides and manganese oxides, which is the reason why in the PCA analysis it appears in a third separated group and it is not included in the dendrite mineralization group together with the results from the black deer. It could be the result of a hematite mixed naturally with Mn oxides, but it looks like it is an intentional addition of chalcophanite to the painting, a Mn oxide that has been also identified in local dendrites and, in consequence, it could be considered a pictorial recipe.

Acknowledgements

This work has been financially supported by Spanish Ministerio de Ciencia e Innovación, in the I+D+i program, as part of the project Mic-Raman Prehistoria "*Microscopía Raman, IR, óptica y electrónica (SEM/EDX) de pinturas rupestres prehistóricas del Arco Mediterráneo de la Península Ibérica. Composición, datación, alteraciones y conservación*" (CTQ2009 12489) and by the University of the Basque Country UPV/EHU (Project UFI11-26 Global Change and Heritage). Technical and human support provided by SGIker (UPV/EHU, MICINN, GV/EJ, ESF) is gratefully acknowledged. We would like to thank the support of José Royo Lasarte, director of Parque Cultural del Río Martín (Ariño, Teruel) and the authorizations to undertake this research from Dirección General de Patrimonio Cultural of the Diputación General de Aragón. And last but not least we show gratitude to our colleagues José M[a] Gavira, Ramiro Alloza, Vicente Baldellou and Ramon Viñas for their collaboration in the research of Los Chaparros rock-shelter.

Notes and references

1 A. Beltrán Martínez and J. Royo Lasarte, in *Corpus de arte rupestre del Parque Cultural del río Martín*, Asociación del Parque Cultural del río Martín. Centro de Arte Rupestre Antonio Beltrán, Zaragoza, Spain, 2005.
2 E. Chalmin, M. Menu and C. Vignaud, *Meas. Sci. Technol.*, 2003, **14**, 1590–1597.
3 E. Chalmin, C. Vignaud, F. Farges and M. Menu, *Phase Transform.*, 2008, **81**, 179–203.
4 M. Sepúlveda, D. Valenzuela, L. Cornejo, H. Lienqueo and H. Rousselière, *Revista de Antropología Chilena*, 2013, **45**, 143–159.
5 E. Chalmin, C. Vignaud and M. Menu, *Appl. Phys. A: Mater. Sci. Process.*, 2004, **79**, 187–191.
6 J. E. Post, *Proc. Natl. Acad. Sci. U. S. A.*, 1999, **96**, 3447–3454.
7 R. M. Potter and G. R. Rossman, *Am. Mineral.*, 1979, **64**, 1219–1226.
8 IGME: Mapa Metalogénico de España - DAROCA. Scale: 1:200.000, Cartographic document, First edn, Servicio de Publicaciones Ministerio de Industria, Instituto Geológico y Minero de España, Madrid, 1974.
9 IGME: MAGNA 50 (2[a] Serie). Hoja 493-Oliete. Scale: 1:50.000, Cartographic document, Instituto Geológico y Minero de España, Madrid, 1977.
10 J. M. Mata-Perelló, F. Climent, P. Alfonso, D. Parcerisa and J. Vilaltella, XII Congreso Internacional sobre Patrimonio Geológico y Minero. "Valorización de elementos geomineros en contexto de los geoparques: libro de actas del XII Congreso Internacional sobre Patrimonio Geológico y Minero: 16a sesión científica de la SEDPGYM", Sociedad Española para la Defensa del Patrimonio Geológico y Minero (SEDPGYM), España, 2011, pp. 307–318.
11 J. M. Mata-Perelló, *Revista de Geologia Sèrie B*, 2012, **596**, 1–13.
12 A. Kudelski, *Talanta*, 2008, **76**, 1–8.
13 M. Maguregui, U. Knuutinen, K. Castro and J. M. Madariaga, *J. Raman Spectrosc.*, 2010, **41**, 1400–1409.
14 I. Martínez-Arkarazo, M. Angulo, L. Bartolomé, N. Etxebarría, M. A. Olazabal and J. M. Madariaga, *Anal. Chim. Acta*, 2007, **584**, 350–359.
15 N. Prieto-Taboada, I. Ibarrondo, O. Gómez-Laserna, I. Martinez-Arkarazo, M. A. Olazabal and J. M. Madariaga, *J. Hazard. Mater.*, 2013, **248–249**, 451–460.
16 J. Moros, A. Gredilla, S. Fdez-Ortiz de Vallejuelo, A. de Diego, J. M. Madariaga, S. Garrigues and M. de la Guardia, *Talanta*, 2010, **82**, 1254–1260.
17 C. Daher, L. Bellot-Gurlet, A. Le Hô, C. Paris and M. Regert, *Talanta*, 2013, **115**, 540–547.
18 J. M. Mata-Perelló, *Revista de Geología Serie B*, 2009, **238 Vol. XX**, 1–12.
19 M. Aurell, B. Bádenas, A. Casas and S. Alberto, *La Geología del Parque Cultural del Río Martín*, Asociación Parque Cultural del Río Martín, Zaragoza, Spain, 2001.
20 M. T. Fernández, F. García, R. Gil, J. C. Gordillo, E. Porcel and J. Royo, *Guía de cavidades y arte rupestre del Parque Cultural del Río Martín*, Centro de Estudios Espeleológicos Turolenses, Asociación Parque Cultural del Río Martín, Teruel, Spain, 2012.
21 K. Castro, M. Pérez-Alonso, M. D. Rodríguez-Laso, L. A. Fernández and J. M. Madariaga, *Anal. Bioanal. Chem.*, 2005, **382**, 248–258.

22 R. T. Downs, *Program and Abstracts of the 19th General Meeting of the International Mineralogical Association in Kobe*, Japan, 2006, pp. O03–13.
23 A. Hernanz, J. M. Gavira-Vallejo, J. F. Ruiz-López, S. Martin, Á. Maroto-Valiente, R. de Balbín-Behrmann, M. Menéndez and J. J. Alcolea-González, *J. Raman Spectrosc.*, 2012, **43**, 1644–1650.
24 A. Hernanz, J. F. Ruiz-López, J. M. Madariaga, E. Gavrilenko, M. Maguregui, S. Fdez-Ortiz de Vallejuelo, I. Martínez, R. Alloza-Izquierdo, V. Baldellou-Martínez, R. Viñas-Vallverdú, A. Rubio i Mora, A. Pitarch and A. Giakoumaki, *J. Raman Spectrosc.*, 2014, DOI: 10.1002/jrs.4535.
25 R. E. M. Hedges, C. Bronk Ramsey, G. J. van Klinken, P. B. Pettitt, C. Nielsen-Marsh, A. Etchegoyen, J. O. Fernández-Niello, M. T. Boschín and A. M. Llamazares, *Radiocarbon*, 1998, **40**, 35–44.
26 J. M. Arocena, K. Hall and I. Meiklejohn, *Geoarchaeol. Int. J.*, 2008, **23**, 293–304.
27 M. J. Beazley, R. D. Rickman, D. K. Ingram, T. W. Boutton and J. Russ, *Radiocarbon*, 2002, **44**, 675–683.
28 A. A. Gorbushina, J. Heyrman, T. Dornieden, M. Gonzalez-Delvalle, W. E. Krumbein, L. Laiz, K. Petersen, C. Saiz-Jimenez and J. Swings, *Int. Biodeterior. Biodegrad.*, 2004, **53**, 13–24.
29 A. Hernanz, J. M. Gavira, J. F. Ruiz and H. G. M. Edwards, *J. Raman Spectrosc.*, 2008, **39**, 972–984.
30 D. Hess, D. J. Coker, J. M. Loutsch and J. Russ, *Geoarchaeology*, 2008, **23**, 3–11.
31 W. E. Krumbein, U. Brehm, G. Gerdes, A. A. Gorbushina, G. Levit and K. Palinska, in *Fossil and Recent Biofilms. A Natural History of Life on Earth*, ed. W.E. Krumbei, D.W. Paterson and G.A. Zavarzin, Kluwer Academic Press Publishers, Dordrecht, 2003, pp. 1–28.
32 M. F. Macedo, A. Z. Miller, A. Dionisio and C. Saiz-Jimenez, *Microbiology*, 2009, **155**, 3476–3490.
33 J. F. Ruiz, A. Hernanz, R. A. Armitage, M. W. Rowe, R. Viñas, J. M. Gavira-Vallejo and A. Rubio, *J. Archaeol. Sci.*, 2012, **39**, 2655–2667.
34 H. G. M. Edwards and T. Munshi, *Anal. Bioanal. Chem.*, 2005, **382**, 1398–1406.
35 N. Cole and A. Watchman, *Antiquity*, 2005, **79**, 661–678.
36 M. Franzini, C. Gratziu and E. Wicks, *Rend. Soc. Ital. Mineral. Petrol.*, 1984, **39**, 59–70.
37 P. Jezequel, G. Wille, C. Beny, F. Delorme, V. Jean-Prost, R. Cottier, J. Breton, F. Dure and J. Desprie, *J. Archaeol. Sci.*, 2011, **38**, 1165–1172.
38 H.-S. Kim and P. C. Stair, *J. Phys. Chem. B*, 2004, **108**, 17019–17026.
39 F. Buciuman, F. Patcas, R. Cracium and D. Zahn, *Phys. Chem. Chem. Phys.*, 1999, **1**, 185–190.
40 L. Beck, H. Salomon, S. Lahlil, M. Lebon, G. P. Odin, Y. Coquinot and L. Pichon, *Nucl. Instrum. Methods Phys. Res., Sect. B*, 2012, **273**, 173–177.
41 E. Chalmin, C. Vignaud, H. Salomon, F. Farges, J. Susini and M. Menu, *Appl. Phys. A: Mater. Sci. Process.*, 2006, **83**, 213–218.
42 E. Chalmin, F. Farges, C. Vignaud, J. Susini, M. Menu and G. E. Brown, *AIP Proceedings of the 13th International Conference On X-Ray Absorption Fine Structure (XAFS13)*, Stanford, California, 2007, pp. 220–222.
43 I. Reiche and E. Chalmin, *J. Anal. At. Spectrom.*, 2008, **23**, 799–806.
44 C. Roldán, S. Murcia-Mascarós, J. Ferrero, V. Villaverde, E. López, I. Domingo, R. Martínez and P. M. Guillem, *X-Ray Spectrom.*, 2010, **39**, 243–250.
45 C. Roldán, V. Villaverde, I. Ródenas, F. Novelli and S. Murcia, *J. Archaeol. Sci.*, 2013, **40**, 744–754.
46 B. Guineau, M. Lorblanchet, B. Gratuze, L. Dulin, P. Roger, R. Akrish and F. Muller, *Archaeometry*, 2001, **43**, 211–225.
47 S. Lahlil, M. Lebon, L. Beck, H. Rousselière, C. Vignaud, I. Reiche, M. Menu, M. P. Paillet and F. Plassard, *J. Raman Spectrosc.*, 2012, **43**, 1637–1643.
48 F. Ospitali, D. C. Smith and M. Lorblanchet, *J. Raman Spectrosc.*, 2006, **37**, 1063–1071.
49 D. C. Smith, M. Bouchard and M. Lorblanchet, *J. Raman Spectrosc.*, 1999, **30**, 347–354.
50 A. Zoppi, G. F. Signorini, F. Lucarelli and L. Bachechi, *J Cult Herit*, 2002, **3**, 299–308.

